PHYSICAL REVIEW B VOLUME 15, NUMBER 4 15 FEBRUARY 1977

Energy bands and bonding in LaB_6 and YB_6†

P. F. Walch
Lewis University, Lockport, Illinois 60441
and Argonne National Laboratory, Argonne, Illinois 60439

D. E. Ellis
Northwestern University, Evanston, Illinois 60201

F. M. Mueller*
Argonne National Laboratory, Argonne, Illinois 60439
(Received 26 July 1976)

Energy bands of the "covalent metal" LaB_6 have been calculated by a discrete variational method in the Hartree-Fock-Slater model. We find that the basic topology of the bands and the predicted Fermi surface are rather insensitive to the atomic configuration assumed in constructing the potential. The proposed Fermi surface is consistent with the basic features of published experimental de Haas–van Alphen data; it is not consistent with the hypothesis of magnetic breakdown which has been invoked to explain the finer details. A study of selected valence-band and conduction-band wave functions supports the conclusion that La-B bonding is more important than La-La bonding in explaining the metallic behavior of LaB_6. The total density of states and the interband joint density of states for several bands are calculated and the results are compared to x-ray and optical data. Preliminary calculations of the energy bands of YB_6 are presented; the similarity of these bands to those of LaB_6 indicates that the relatively high superconducting transition temperature of YB_6 cannot be explained by simple density-of-states arguments.

I. INTRODUCTION

Lanthanum hexaboride is one of a series of extremely hard, refractory, and stable MB_6 materials characterized by strong covalent bonds.[1] Semiempirical theoretical models predict that the trivalent lanthanum ion will cause the compound to be metallic.[2] Studies of the optical and electrical properties of LaB_6 have shown this to be the case.[3,4] LaB_6 is a good thermionic emitter finding current usage as an electron microscope cathode.[5,6] This compound has been found to be a superconductor having a quite low transition temperature of 0.45 K, while YB_6 has a relatively high T_c of 7.1 K.[7]

Previous theoretical studies have primarily used semiempirical molecular-orbital models to explain the bonding characteristics and metallic behavior of LaB_6.[2] A more quantitative theory is required to describe spectroscopic or transport properties. We have previously reported preliminary results of a band-structure calculation for this material.[8] In addition, band-structure calculations have been reported for semiconducting calcium hexaboride,[9] and for a series of metal hexaborides.[10]

In this paper we present the results of several first-principles energy-band calculations for LaB_6, along with preliminary results for YB_6. We shall be interested in using these results to gain a better understanding of the metallic behavior and great rigidity of such materials. The remainder of the paper is arranged as follows. In Sec. II we discuss the Hartree-Fock-Slater model and our computational method. A discussion of the energy bands is presented in Sec. III. In Sec. IV, the crystal wave functions are examined in relation to the bonding of LaB_6. Comparison of our results with experimental data, and a discussion of some preliminary results for YB_6 is found in Sec. V, and we give our conclusions in Sec. VI.

II. THEORETICAL MODEL AND COMPUTATIONAL METHOD

In this work we examine the predictions of the Hartree-Fock-Slater (HFS) model for the occupied levels and low-energy excitations of LaB_6, adopting the simplest one-electron direct-transition interpretation of the excitation spectrum. Thus the effective Hamiltonian is

$$H = T + V_C + V_x ,$$

where the first two terms are the kinetic energy and Coulomb potential, respectively, and the exchange operator V_x is approximated by the local potential (in Hartree atomic units)

$$V_x = -3\alpha(3\rho/8\pi)^{1/3} .$$

Various theoretical prescriptions for selection of a value for the adjustable parameter α have been presented in the literature.[11-14] The current calculations were performed both with $\alpha = 1.0$ and 0.7

in order to investigate effects of the exchange approximation on properties like the Fermi surface. The crystal charge density ρ is approximated by the superposition of atomic (ionic) densities as

$$\rho = \sum_{\nu} \rho_{\nu} ,$$

and the Hamiltonian is thus determined. We make some effort to "bracket" the results which would be obtained from complete self-consistent-field calculations (see Sec. III) by considering several possible input atomic configurations. It is important to note that the full crystal potentials are determined, without making the usual muffin-tin averaging approximations; thus all aspherical "crystal-field" terms are retained. When the potential is approximated by its muffin-tin average, the Schrödinger equation is separable within each sphere, and the first-principles augmented-plane-wave and Kohn-Korringa-Rostocker methods can be more easily applied.[15] This model of the potential, while adequate for most metals, is often a serious oversimplification when one is treating nonmetals and compounds.[16-18] For example, the crystal potential of LaB_6 is quite aspherical, as shown in Fig. 1.

In the present work, approximate eigenvalues and eigenfunctions of the HFS Hamiltonian are generated by means of a discrete variation method which has been previously applied to a number of energy-band problems.[16,17] These calculations involve the selection of a discrete set of sample points in coordinate space, and minimization of an error functional over the grid of sample points by a variational procedure. These direct numerical-variational techniques have been used with considerable success in treating potentials of very general form; detailed discussions may be found elsewhere.[18,19]

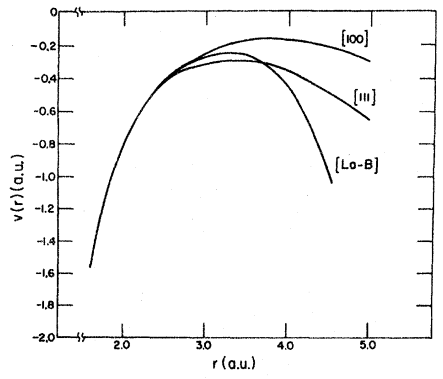

FIG. 1. Angular variation of crystal potential around lanthanum site. La-B represents the nearest-neighbor bond direction. The crystal potential was calculated from a d^1s^2 lanthanum configuration.

The approximate wave functions are expanded in a fixed basis set

$$\psi_i(\vec{k}, \vec{r}) = \sum_j \chi_j(\vec{k}, \vec{r}) C_{ji}(\vec{k}) ,$$

where the basis functions $\chi_j(k, r)$ are Bloch orbitals of wave vector $\vec{k}$ belonging to the $\vec{k}$th irreducible representation of the crystal translation group. The basis orbitals are in turn constructed here from unsymmetrized linear combinations of Slater-type orbitals (STO's) centered at nuclear sites. This linear-combination-of-atomic-orbitals basis is most efficient for forming crystal wave functions for those systems in which the atomic character of the constituent atoms is maintained to a large degree. Systems in which the bonding between atoms is strong and highly directional are very conveniently described in terms of this basis, since a connection can be made to molecular-orbital bonding schemes.

III. ENERGY BANDS FOR LaB_6

The crystal structure of LaB_6 is shown in Fig. 2. Bands were calculated for the room-temperature lattice constant of 7.853 a.u.[1] Considerable experimentation was done by varying the number and type of STO's centered on the lanthanum and boron sites to determine the effects of basis truncation on the band energies. All LaB_6 bands discussed here were generated using the STO basis shown in Table I; this 134 function set represents a reasonable compromise between accuracy and computational cost. There are ten boron basis functions of roughly "double zeta[20]" quality, on

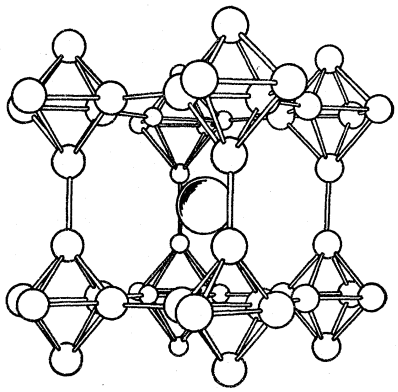

FIG. 2. Crystal structure of MB_6 (M is a metal ion) with the three-dimensional framework of interlocked B_6 octahedra shown in perspective surrounding the metal ion. Crystal structure is the CsCl type (O_h^1) with seven atoms per unit cell. The lattice constant is 7.853 a.u. for LaB_6 and 7.752 a.u. for YB_6. (Reprinted from Ref. 1 with permission.)

TABLE I. STO basis functions for LaB_6 energy bands.

nl	ζ	nl	ζ
	Lanthanum		
$1s$	60.0	$4s,p,d$	4.5
$1s$	40.0	$5s,p,d$	4.0
$2s,p$	30.0	$5s,p$	2.9
$2s,p$	13.0	$6s,d$	2.5
$3s,p,d$	11.0	$6p$	2.0
$3s,p,d$	7.5	$8s,d$	2.5
$4s,p,d$	7.5		
	Boron		
$1s$	8.0	$2s,p$	3.7
$1s$	4.5	$2s,p$	2.2

TABLE II. Characteristics of sample point mesh.[a]

Site	Radius (a.u.)	No. of points
Lanthanum (sphere)	1.5	1300
Boron (6 spheres)	1.668	200/atom
Interstitial[b]	...	1472

[a] The crystal unit cell was divided into seven atomic regions and an interstitial region. In each atomic region N_a quasirandom points were generated by a Diophantine procedure (Refs. 18 and 19) with uniform radial density. The interstitial region was sampled with N_i quasirandom points.

[b] Interstitial region comprises 74% of the unit cell volume.

each ligand site. The lanthanum basis includes seven sets of d orbitals but no f orbitals. After considerable testing, f-orbital contribution to energies near the Fermi surface was deemed to be inconsequential in comparison to lanthanum d-orbital and ligand-orbital contributions. Convergence of band energies as a function of the number of sampling points per cell (numerical integration grid) was also investigated. A 3972-point mesh, which is described in Table II, was found capable of giving sufficient accuracy at reasonable cost. The small metal sphere radius was chosen in order that the resulting high density of points would lead to an adequate description of the complicated wave-function behavior near the lanthanum nucleus. The large number of interstitial sampling points made it possible to adequately converge the diffuse $5d$- and $6s$-lanthanum orbital contribution to the Bloch functions.

The energy bands for LaB_6 are plotted along the usual symmetry directions in Figs. 3 and 4; results for several different potentials are shown in order to explore sensitivity to the assumed crystal potential. In all calculations, the input lanthanum charge density and Coulomb potential was derived from numerical HFS free-atom wave functions; the corresponding boron quantities were derived from Hartree-Fock free-atom wave functions. The calculated energies are estimated to be converged to within ±0.003 Ry.

The energy bands were calculated at 18 k points. This number was judged to be suitable for an adequate understanding of the Fermi surface and the density of states. Computer time per k point on the IBM-360/195 at Argonne National Laboratory was about 1000 sec of CPU (central processor unit) time. Fifteen of the k points were chosen to lie along high-symmetry directions and three were points of lowest symmetry. An approximate balance of k-space volume per point was achieved by spreading the points on or near the $k=0$, $\pi/4a$, $\pi/2a$, $3\pi/4a$, π/a planes in numbers roughly proportional to the planar area.

In Fig. 3, a set of bands using the Hamiltonian generated from the neutral atom configurations: La : $5d^16s^2$, B : $2s^22p^1$ is shown by the solid lines while a set of selected eigenvalues calculated from the neutral atom configurations: La : $5d^26s^1$, B : $2s^22p^1$ is shown by the dotted lines. An exchange parameter $\alpha=1.0$ was used for both calculations. Figure 4 represents the energy bands calculated from the d^1s^2 neutral atom configuration but with $\alpha=0.7$. The lessened value of exchange results in bands which are slightly flatter than but topologically similar to those in Fig. 4. Thus, we find that different plausible starting potentials for the HFS model lead to essentially the same band structure and Fermi surface. It is clear from the differences observed that complete quantitative agreement with experimental Fermi surface parameters could be expected only for full self-consistent calculations which are at present prohibitively expensive.

In an attempt to further understand the low value

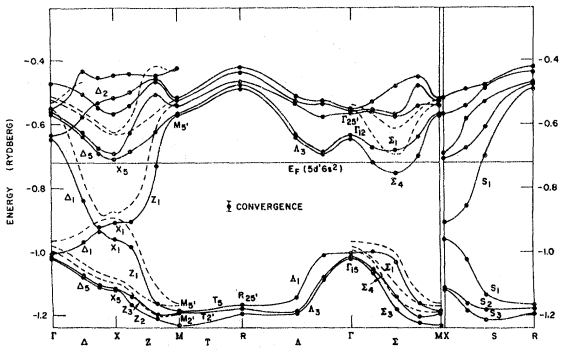

FIG. 3. Electronic energy-band structure of LaB_6 for $\alpha=1$. The complete bands for the d^1s^2 potential are shown by the solid lines; the partial bands for the d^2s^1 potential are indicated by the dotted lines.

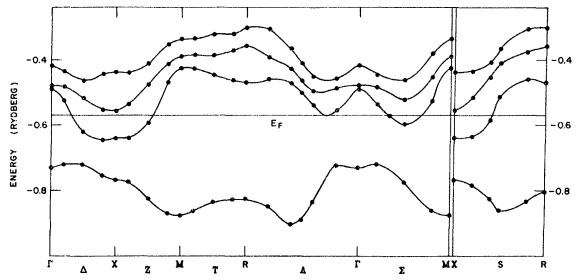

FIG. 4. Electronic energy band structure of LaB_6 for $\alpha = 0.7$. The assumed lanthanum atom state is $5d^16s^2$.

of T_c for LaB_6 we have performed preliminary band calculations for YB_6, a conductor having the much higher T_c of 7.1 K.[7] The results shown in Fig. 5 for $\alpha = 1.0$, were obtained with a sample point mesh of 3595 points using a 115 function basis set similar to the one used for LaB_6. It is to be noted that the bands of YB_6 are very similar to the bands of LaB_6.

IV. WAVE FUNCTIONS AND BONDING

Previous theoretical studies[2] have centered on the bonding between the boron atoms that make up each octahedron and also on the octahedron-octahedron bonding required to hold the cage together. Supposedly, the metal atom is unimportant to the stability of the cage, a view which is supported by the similarity of the lattice constants for the entire MB_6 isostructural series.[1] An extreme result of this viewpoint is Lafferty's conclusion[6] that the high efficiency of LaB_6 emitters results from the ability of lanthanum atoms to migrate through the boride matrix in order to replace lanthanum atoms evaporated from the surface. In this section, the LaB_6 crystal wave functions will be examined and the importance of lanthanum-boron bonding will be emphasized.

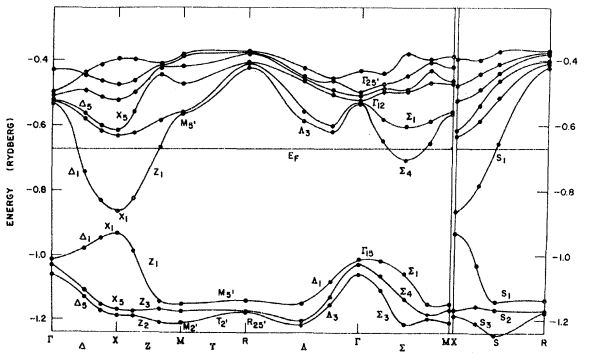

FIG. 5. Electronic energy-band structure for YB_6 using $\alpha = 1$. The crystal potential was generated from free atom configurations: $Y: 4d^15s^2$, $B: 2s^22p^1$.

Crystal wave functions were calculated for the Γ, X, M, and R points in k space. The Γ wave functions provide an interesting comparison to the molecular-orbital description of Longuet-Higgins and Roberts.[2] The occupied Γ_{15} bonding level at ~ -1 Ry is made up of a linear combination of mainly $2p$-orbitals centered on the boron sites along with some $5d$ contribution from the lanthanum. The unoccupied Γ_{12} wave function at ~ -0.6 Ry has typical La-$5d$ character as well as some B-$2p$ behavior. Results of a population analysis,[21] in which the overlap population was arbitrarily divided evenly between the lanthanum atom and the B_6 complex, show the occupied Γ_{15} state to be 23% lanthanum and 77% boron in character. The intuitive picture of trivalent lanthanum is thus vindicated. As expected, the first conduction level is d-like and primarily centered on the La atom. The energy separation of the (unoccupied) Γ_{12} and Γ'_{25} states is an indication of crystalfield effects which may be observed in optical absorption data.[1] The crystal-field parameter parameter Δ is ~1.1 eV (Fig. 3) and the ordering is indicative of the cubic O_h symmetry provided by the eight $(B_6)^{-3}$ complexes which surround each lanthanum ion (Fig. 2). It is interesting to compare this result to that for the energy bands of $LaSn_3$. In the latter case, Gray and Meisel, found $\Delta \sim 0.7$ eV with Γ_{12} above Γ'_{25}.[22]

The angular dependence of the Γ wave functions is somewhat complicated. As expected, the principal maxima of the p-function in Γ_{15} and the d function in Γ_{12} are most extended in the boron direction. In fact, the outer maxima essentially disappear in the [100] or La-La direction (La-La distance is 7.853 a.u.). Hence, we conclude that La-La bonding is relatively unimportant in comparison to La-B bonding (La-B distance is 5.774 a.u.), and the ordering of the Γ_{12}, Γ'_{25} levels is not due to the crystal field of the six positive lanthanum ion ligands (octahedral O_h symmetry).

This view is further strengthened when one examines the X_1 (X_5) wave functions representing states below (above) the Fermi energy. It is interesting to note that the bonding charge represented by the X-point wave functions is greater in the [111] direction than in the boron direction, since the lanthanum atom is bonding to a hybridized complex of s-p orbitals from the entire B_6 "cage." Results of a population analysis indicate the following metal character: X_1 (valence)—64%, X_1 (conduction below E_F)—98%, X_5 (above E_F)—52%.

From these observations, it is clear that there is significant bonding between the lanthanum and boron atoms. Contrary to the semiempirical results of Perkins *et al.*,[10] we find no evidence of a broadening of the valence bands due to La-La

s-orbital overlap. The highest-energy valence band we find with predominantly La-s character is ~0.5 eV wide and lies well below the bands shown in Figs. 3 and 4; Perkins *et al.*[10] show this band to be over 10 eV wide. The results reported here confirm the semiempirical results of Longuet-Higgins and Roberts[2] that electrons from the La atom serve to stabilize the boron framework. If we crudely estimate that the highest valence bands are 44% lanthanum (based on an average of the population analysis for Γ and X states), the integrated lanthanum charge totals 2.64 in rough agreement with the predicted value of 2.0 electrons required for stabilization of the boron framework.[2]

Wave functions for the conduction levels Γ_{12} and X_5 show little evidence of La-La overlap. Probably the high conductivity of LaB_6 is mainly due to the La-B bonding and not to the weaker La-La bonding. It is satisfying to note that this view of La-B bonding in LaB_6 has received partial confirmation in the work of Ahmed and Broers.[6] After a careful examination of LaB_6 emitters *in situ*, they concluded, contrary to Lafferty, that preferential lanthanum evaporation does not occur at the surface; it appears that both lanthanum and boron atoms evaporate together.

V. COMPARISON WITH EXPERIMENT

A. de Haas–van Alphen data

Several studies of the Fermi surface of LaB_6 using the de Haas–van Alphen effect (dHvA) have been reported.[8,23,24] Aided by preliminary energy band calculations,[8] Arko *et al.*[8,23] interpreted much of their data as being consistent with a set of nearly spherical ellipsoids located at the point X in the Brillouin zone and connected by necks which intersect the ΓM line. Magnetic breakdown across the necks had to be postulated to explain the remaining data.

The results of the band calculations shown in Figs. 3 and 4 have the basic topology required to explain the experimental results. The Fermi energy E_F cuts only a single band. Near the symmetry point X we note that there is an electron surface centered at X which is closed along the $X\Gamma$ (Δ_1) and XM (Z_1) directions. We also note that the Σ_4 level intersects the Fermi energy in the ΓM direction; this is required if there are to be necks connecting the X centered ellipsoids. The complete band calculations for $\alpha = 1.0$ and 0.7, using the d^1s^2 potential both give this basic topology. The location of E_F for the calculation of partial bands using the d^2s^1 potential (dotted lines in Fig. 3) is uncertain; however, the basic topology around X and along Σ is so similar to the other calculations that the ball-neck geometry is undoubtedly preserved for this case also.

Comparison of the experimental[8,23] and theoretical values for the extremal cross-sectional areas and effective masses in LaB_6 will be found in Table III. The notation is that of Arko *et al.*,[23] χ_1 represents the electron ball orbit normal to [100], while γ and μ represent hole orbits centered at Γ and M, respectively. Quantitative agreement between theory and experiment is not found; both band calculations give effective masses for a principal ball orbit which are quite low compared to experiment.

In order to explain several dHvA frequencies and the experimental magnetoresistance results, magnetic breakdown across the necks must be invoked. However, the calculated bands show the Fermi surface to be constructed from a single sheet, namely, the fourth band in Figs. 3 and 4. Nowhere in the vicinity of the necks (Σ direction) do the energies of two different bands become sufficiently close for magnetic breakdown to have a reasonable probability of happening. Calculations of band energies normal to the Σ symmetry direction indicate that the necks are probably more round than those envisioned in the experimental model.[8,23]

TABLE III. Cross-sectional area and effective-mass data for LaB_6.

	Branch[a] (normal to [100])	Experimental[b]	Band structure $\alpha = 1.0$	Band structure $\alpha = 0.7$
Area (in a.u.)	χ_1	0.211	0.21	0.15
	γ			0.06
	μ			0.12
Mass m^* (in a.u.)	χ_1	0.61	0.29	0.40
	γ			0.37
	μ			0.61

[a] Notation of Ref. 23, χ_1 represents the electron ball orbit normal to [100], γ and μ represent hole orbits centered at Γ and M, respectively.

[b] Reference 23.

Thus, the calculated Fermi surface gives a reasonable explanation of the basic features of the dHvA data while failing to explain the finer details. Recently, an alternate Fermi surface has been proposed by Perkins, Armstrong, and Breeze.[10] Their Fermi surface consists of three sheets with two closed pieces centered at Γ and a multiply connected "jungle gym" of cylinders running along [100] and meeting at Γ. This model fails to explain the experimental data.[23] On the other hand Ishizawa *et al.*[24] independently deduced the same experimental Fermi surface as that of Arko *et al.*[8,23]

Comparison of the energy bands of YB_6 with experimental data is not yet possible due to the lack of sufficiently high stoichiometry in the crystals for dHvA measurements.[25] The Fermi energy again intersects a single band and a ball-neck Fermi surface is predicted (Fig. 5).

B. Density of states and T_c

The density of states of LaB_6 and YB_6 is shown in Fig. 6. The densities of states were calculated by straightforward procedures discussed in detail elsewhere.[17] The optimum number of symmetrized sum of plane-wave-fitting functions was 13 for bands computed at 18 inequivalent k points. The resulting rms errors in the energy-band fits were no worse than 0.005 Ry in the valence bands, 0.006 Ry in the Fermi band, and 0.01 Ry in the conduction bands. Both compounds exhibit a high density of states in the bonding band and in the antibonding band above the Fermi energy. The Fermi level lies in the middle of a broad conduction band. The calculated density of electronic states at E_F is 5.01 states/Ry for LaB_6 and 6.05 states/Ry for YB_6. These results are sufficiently similar to apparently rule out the factor of ~15 difference in T_c as due to simple density-of-states effects. It now appears desirable to consider the phonon spectra and/or lattice defect structure for further enlightenment.[8]

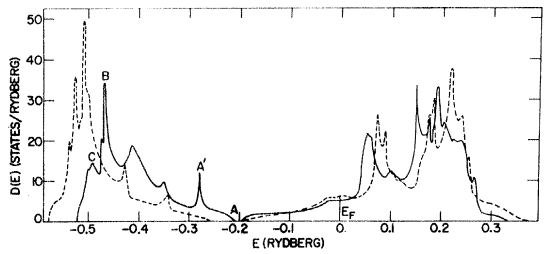

FIG. 6. Density of states for LaB_6 (solid line) and YB_6 (dashed line). Results have been aligned to give a common value of E_F and are derived from the $\alpha = 1$ band calculations using a d^1s^2 potential.

C. Optical and x-ray data

The calculated density of states was compared to the experimental boron K x-ray emission data[26] for LaB_6. The K emission spectrum does not give the density of p valence states directly since all transition probabilities are not necessarily equal. However, the assumption of constant transition probabilities is a reasonable first approximation given the dominant boron p character of the valence bands. It is not possible to compare the boron K absorption spectrum with the calculated density of states because we have not broken down the total density of states into orbital contributions. The peaks in Fig. 6 are labeled to correspond to the x-ray data of Lyakov-skaya *et al.*[26] With this convention the calculated separations are: A-A', 1.0 eV; A'-B, 2.6 eV; B-C, 0.4 eV. The corresponding experimental splittings are 1.1, 2.9, and 1.1 eV; unlabeled peaks in the density of states are not resolved in the experimental data.

In order to obtain a qualitative understanding of the optical absorption data for LaB_6 the interband density of states d_{ij} was calculated for several pairs of bands.[17]

$$d_{ij}(E) = \frac{2}{(2\pi)^3} \int d^3k\, \delta(E_{ji}(\vec{k}) - E),$$

where $E_{ji} = E_j - E_i$. We use the $\vec{k}$ selection rule (direct interband transitions), in the "constant oscillator strength" approximation to discuss individual band-pair contributions to the optical reflectivity. The amplitudes in the conventional histogram representation were calculated by diophantine sampling[17] using 8000 sample points. The results are plotted in Fig. 7 for the transitions

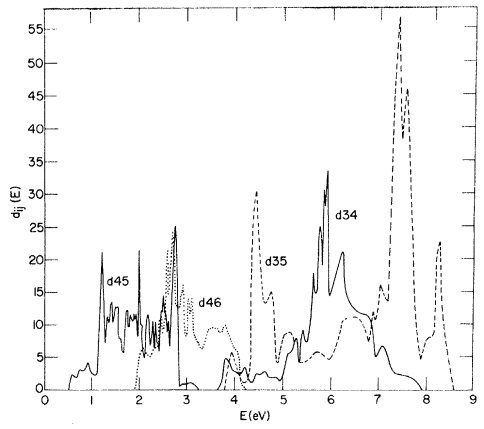

FIG. 7. Interband joint density of states for the $\alpha = 1$ band calculation for LaB_6 using the d^1s^2 potential. The bands are numbered in the order in which they appear in Fig. 3.

$3 \rightarrow (4,5)$ and $4 \rightarrow (5,6)$ where band 3 is the highest valence band and band 4 is cut by E_F (Fig. 3). In view of the fact that the bands were only calculated at 18 k points, some of the structure in Fig. 7 is probably due to noise. The discussion will be limited to an analysis of the major peaks.

Any contribution from interband $4 \rightarrow 5$ transitions is masked by the strong intra-band transitions below the plasma edge at 2.1 eV.[4] The lowest interband transition is experimentally uncertain,[4] but our results show a large value in both d_{45} and d_{46} at an energy slightly above the plasma edge. This may contribute to the rapid rise in the experimental reflectivity for photon energies slightly above 2.1 eV. The experimental reflectance data shows peaks at 4.9 and 5.4 eV; no data are available above about 5.7 eV.[4] The experimental peaks at 4.9 eV may correspond to the dominant peak at ~4.5 eV in d_{35}. This peak is probably associated with transitions over a considerable region of k space extending outward from the zone center (Γ point) in the Λ and Σ directions. The experimental peak at 5.4 eV can be correlated with the large peak at ~5.9 in d_{34}, due to a large k volume of transitions to states just above E_F notably along Z, Λ, Σ, and S. It is interesting to note that the interband density of states calculations also predict a strong transition at ~7.5 eV and a weaker one at ~8.3 eV.

It is apparent that a good qualitative understanding of the optical properties of LaB_6 result from these calculations of d_{ij}. Better agreement is to be anticipated when the oscillator strengths are computed and a theoretical value of the imaginary part of the dielectric constant is calculated.

VI. CONCLUSIONS

We have examined the HFS energy bands for LaB_6 and YB_6 and found a striking similarity in the results; this similarity persists even through wide variations in the crystal potential. The proposed Fermi surface for both materials is of the ball-neck type and agreement with the basic details of the experimental dHvA results is good. These basic results would probably be substantiated by a full self-consistent-field band calculation. Semiquantitative arguments are advanced to support the conclusion that La-B bonding is more important than La-La bonding in explaining the metallic behavior of LaB_6. The failure of our calculations to explain the relatively high T_c of YB_6 demonstrates the need to explore the phonon spectrum more carefully. Finally, satisfactory agreement between theory and experiment is found for the x-ray and optical data of LaB_6.

ACKNOWLEDGMENTS

We gratefully acknowledge the help and stimulus provided by Dr. A. J. Arko, Dr. G. Crabtree, Dr. Z. Fisk, Dr. A. J. Freeman, Dr. J. B. Ketterson, and Dr. D. D. Koelling.

---

†Work supported by USERDA, AFOSR, and NSF (through Northwestern University Materials Research Center).

*Present address: Faculty of Science, University of Nijmegen, Toernooiveld, Nijmegen, The Netherlands.

[1]*The Chemistry of Boron and Its Compounds*, edited by E. L. Muetterties (Wiley, New York, 1967).

[2]H. C. Longuet-Higgens and M. de V. Roberts, Proc. R. Soc. Lond. A 224, 336 (1954); W. N. Lipscomb and D. Britton, J. Chem. Phys. 33, 275 (1960).

[3]E. Kauer, Phys. Lett. 7, 171 (1963).

[4]E. Kierzek-Pecold, Phys. Status Solidi 33, 523 (1969).

[5]Phys. Today 27, 17 (1974).

[6]J. M. Lafferty, J. Appl. Phys. 22, 299 (1951); H. Ahmed and A. N. Broers, *ibid.* 43, 2185 (1972).

[7]J. M. Vanderberg, B. T. Matthias, E. Corenzwit, and H. Borz, Mater. Res. Bull. 10, 889 (1975).

[8]A. J. Arko, G. Crabtree, J. B. Ketterson, F. M. Mueller, P. F. Walch, L. Windmiller, Z. Fisk, R. Hoyt, A. Mota, R. Viswanathan, D. E. Ellis, A. J. Freeman, and J. Roth, Int. J. Quant. Chem. Symp. 9, 569 (1975).

[9]M. Yamazaki, J. Phys. Soc. Jpn. 12, 1 (1957).

[10]P. G. Perkins, D. R. Armstrong, A. Breeze, J. Phys. C 8, 3558 (1975).

[11]J. C. Slater, Phys. Rev. 81, 385 (1951).

[12]W. Kohn and L. J. Sham, Phys. Rev. 140, A1133 (1965).

[13]R. Gaspar, Acta Phys. Acad. Sci. Hung. 3, 263 (1954).

[14]I. Lindgren, Ark. Fys. 31, 59 (1965); Phys. Lett. 19, 382 (1965).

[15]Methods in Computational Physics, edited by B. Adler, S. Fernbach, and M. Rotenberg (Academic, New York, 1968), Vol. 8. Recently, the "warped-muffin-tin" approximation has been used to correct some of the defects in standard muffin-tin calculations; cf. D. D. Koelling, A. J. Freeman, and F. M. Mueller, Phys. Rev. B 1, 1318 (1970); B. N. Harmon, D. D. Koelling, and A. J. Freeman, J. Phys. C 6, 2294 (1973).

[16]G. S. Painter and D. E. Ellis, Phys. Rev. B 1, 4747 (1970); D. E. Ellis and G. S. Painter, *ibid.* 2, 2887 (1970).

[17]P. F. Walch and D. E. Ellis, Phys. Rev. B 8, 5920 (1973); G. S. Painter, D. E. Ellis, and A. R. Lubinsky, *ibid.* 4, 3610 (1971); A. R. Lubinsky, D. E. Ellis, and G. S. Painter, *ibid.* 11, 3131 (1975).

[18]D. E. Ellis and G. S. Painter, in *Computational Methods in Band Theory*, edited by P. M. Marcus, J. F. Janak, and A. R. Williams (Plenum, New York, 1971), p. 271; G. S. Painter and D. E. Ellis, *ibid.*, p. 276.

[19]D. E. Ellis, Int. J. Quant. Chem. Symp. 2, 35 (1968); G. S. Painter and D. E. Ellis, *ibid.* 3, 801 (1970).

[20]E. Clementi, IBM J. Res. Dev. Suppl. 9, 2 (1965).

[21]R. S. Mulliken, J. Chem. Phys. 23, 1833 (1955).

[22]D. M. Gray and L. V. Meisel, Phys. Rev. B 5, 1299 (1972).
[23]A. J. Arko, G. Crabtree, D. Karim, F. M. Mueller, L. R. Windmiller, J. B. Ketterson, and Z. Fisk, Phys. Rev. B 13, 5240 (1976).
[24]Y. Ishizawa, T. Tanaka, S. Kawai, and E. Bonnai, *Proceedings of the Fourteenth International Conference on Low Temperature Physics* (Helsinki U. P., Finland, 1975).
[25]A. J. Arko and Z. Fisk (private communication).
[26]I. I. Lyakovskaya, T. M. Zimkina, V. A. Fomichev, Sov. Phys.-Solid State 12, 138 (1970).